Article

Toba-CPD: An Extended Chemical Percolation Devolatilization Model for Tobacco Pyrolysis

Hao Wei, Yuhan Peng, Hua Huang, Jianqi Fan, Jiangkuan Xing,* Kun Luo,* Jianren Fan, and Lu Dai

Read Online

ACCESS | Metrics & More | Article Recommendations

ABSTRACT: Tobacco features chemical compositions different from that of raw lignocellulosic biomass. Currently, the performance of network models, like Bio-Chemical Percolation Devolatilization (Bio-CPD), on tobacco pyrolysis is unclear, and only global kinetics have been proposed for tobacco devolatilization, which does not have the versatility for a wide range of heating conditions and tobacco types. To address this issue, the present work first assessed the performance of the Bio-CPD model on tobacco pyrolysis through an *a priori* study, which showed large deviations. Afterward, an extended Chemical Percolation Devolatilization model for tobacco pyrolysis (Toba-CPD) was developed by modifying the kinetic parameters using a grid-search optimization strategy. The process of grid-search optimization strategy is based on the kinetic parameters of the Bio-CPD model and modified with experimental results of 11 tobacco types under a wide range of heating rates. Finally, the performance of Toba-CPD was measured with experimental results which were not used during parameters optimization. Results demonstrated that the Toba-CPD models could well reproduce the pyrolysis of various tobacco types under a wide range of heating rates ($R^2 > 0.957$).
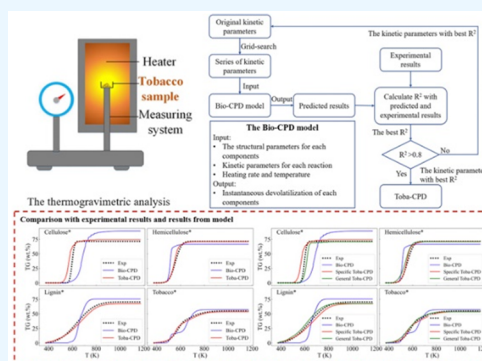
1. INTRODUCTION

There is a large amount of tobacco produced worldwide.[1] Most tobacco is used for producing cigarettes, which is very unhealthy.[2] Hence, there is an urgent need to find other possible uses for tobacco instead of producing cigarettes. Tobacco could be utilized by thermochemical and biochemical routes, such as gasification, combustion, and carbonation, in which pyrolysis is always the primary step.[3−5] Therefore, it is necessary to study the pyrolysis behavior of tobacco and then establish accurate pyrolysis models, which is significant for developing healthy utilization technologies of tobacco.

Tobacco is a plant material and consists of some 3800 constituents, ranging from small organic and inorganic molecules to biopolymers.[6,7] Owing to the importance of an in-depth understanding of tobacco's pyrolysis, considerable researches are focusing on this topic. Experimental methods, such as gas chromatography/mass spectrometry (Py-GC/MS),[8,9] thermogravimetric analyzer coupled with Fourier transform infrared spectrometry (TG-FTIR),[9−11] macro-thermogravimetric (macro-TGA),[8] and thermogravimetric mass spectrometry (TG-MS)[8,9] were usually used to investigate the pyrolysis of tobacco, including studying the effect of oxygen on in situ evolution of chemical structures during tobacco's pyrolysis,[8] finding the pyrolysis character and major pyrolysis products,[9] investigating the effect of different tobacco particle sizes on pyrolysis,[12] and revealing how the volatile products formed.[10] Compared with experimental studies, there have been fewer studies establishing models for

tobacco pyrolysis. Chen et al.[13] proposed a mathematical model for smoldering cigarettes, including the char combustion processes, the pyrolysis of virgin tobacco, and evaporation of water. However, the model can only be used for predicting the temperature and density profiles in smoldering cigarettes, and its performance on other tobacco types and heating conditions was unclear. Encinar et al.[14] established a kinetic model for pyrolysis (including maize, sunflowers, grape, and tobacco) from gas generation by experiment. However, the model assumed the generation of gases during the pyrolysis was a series of independent first-order parallel reactions, which is far from reality. Gao et al.[15] calculated the best linearity of different reaction models for fitting the Coats-Redfern equation from experimental data. However, tobacco pyrolysis is a very complicated chemical reaction process, which can not be well represented by one global reaction or simple reaction combination.

In summary, the established tobacco pyrolysis kinetics usually using global reaction kinetics, which works well for the selected tobacco types and heating conditions. But there is a

lack of an accurate model which could well reproduce the tobacco pyrolysis behaviors for a wide range of tobacco types and heating conditions. On the other hand, tobacco could be regarded as a special type of biomass with different chemical compositions.[6,7] Regarding the modeling of biomass pyrolysis, there have been some advanced network models reported, such as the biochemical percolation devolatilization model (Bio-CPD),[16−18] functional group-depolymerization vaporization cross-linking,[19] and FLASHCHAIN models.[20] These well-established network models worked well for common biomass types, but their performances on tobacco pyrolysis are still unclear. As regard to the Bio-CPD model, it was developed for biomass pyrolysis by Fletcher et al.,[16−18] and can be used to study the pyrolysis mechanism of the major biomass constituents.[21] Actually, the Bio-CPD model was extended from the coal CPD model to model the pyrolysis of hardwood, softwood, kraft, xylan, and glucomannan.[22] The extension was made by retaining the reaction scheme and modifying both the structural parameters and the reaction kinetics parameters for the three major biomass components. But the performance of the Bio-CPD model on the tobacco pyrolysis is unclear. Considering the previous successful extension of the coal CPD model to the Bio-CPD model, it is a reasonable choice and route to further extend the Bio-CPD to the Toba-CPD for tobacco pyrolysis.

Based on the above backgrounds, the aim of the present work is to develop an extended CPD model for tobacco pyrolysis, named the Toba-CPD model. In this model, the general reaction scheme was kept the same as that of the Bio-CPD model, but the kinetic parameters of the reaction routines were modified by a grid-search optimization strategy with the experimental data (various tobacco types and heating conditions) as benchmarks. The present work followed the following steps. First, the pyrolysis process of 11 kinds of tobacco under a wide range of heating rates (10−500 K/min) were measured through TGA and then used to establish a pyrolysis database for the development and validation of the Toba-CPD model. Second, the performance of the traditional Bio-CPD model was accessed through the *a priori* study on the established database. Third, a grid-search optimization method was used to alter the kinetic parameters of the traditional Bio-CPD model to obtain a set of general kinetic parameters for a wide range of heating rates and tobacco types, furthermore developing the Toba-CPD model for a specific tobacco and general tobaccos. Finally, the model performance was confirmed by the *a posteriori* analysis on the unseen tobacco and heating rates.

The rest of this paper is organized as follows. The information on tobacco samples, the experimental methods, and the algorithms of CPD and Toba-CPD models are introduced in section 2. Section 3 presents and discusses the results and discussion, including the *a priori* study of the Bio-CPD model on tobacco pyrolysis, and the performances of the specific Toba-CPD and general Toba-CPD models in predicting tobacco pyrolysis on seen and unseen data sets. The final section provides some concluding remarks.

2. MATERIALS AND METHODS

In this section, information on tobacco samples, and experiment methods are introduced. Then the basic theory and formulas of the CPD model are briefly introduced. Finally, the grid-search optimization strategy is introduced.

2.1. Experimental Methods. In the present study, in total 11 tobacco samples were studied in the experiments. The chemical analysis of each tobacco sample was done to specify the difference of different tobacco sample. The chemical analysis information, including total sugar (TS), starch (ST), reducing sugar (RS), chlorine (Cl), potassium (K), and nitrogen (N), were measured by a continuous flow analyzer (Alliance-Futura), as listed in Table 1. The sugar, starch,

Table 1. Chemical Analysis of the Tobacco Sample

Sample	Sugar (%)	Starch (%)	Reducing Sugar (%)	Cl (%)	K (%)	N (%)
1	33.08	2.38	28.43	0.45	1.94	1.84
2	27.38	2.64	24.37	0.85	1.95	1.94
3	35.32	2.31	30.42	0.29	1.74	2.08
4	32.09	2.66	26.70	0.49	1.73	1.86
5	29.37	2.29	23.85	0.29	2.26	1.71
6	31.19	2.28	27.74	0.48	2.49	1.80
7	37.10	2.25	31.25	0.27	1.53	1.95
8	35.54	2.57	30.35	0.31	1.57	1.98
9	31.10	2.27	27.73	0.48	2.50	1.85
10	34.62	2.11	27.29	0.59	1.65	2.09
11	30.59	1.97	26.56	0.75	1.34	1.59

reducing sugar, Cl, K, and N contents of the 11 samples range from 27.38%−37.10%, 1.91%−2.66%, 24.37%−30.42%, 0.27%−1.85%, 1.34%−2.50%, and 1.59%−2.09%. The measurement uncertainty of TS, ST, RS, Cl, K, and N is ±0.52%, ±0.04%, ±0.62%, ±0.014%, ±0.06%, and ±0.04%, respectively.

From the perspective of the tobacco industry, chemical analysis is very important and widely used to describe the tobacco samples owing to the strong relation between chemical analysis and the quality of tobacco. So, herein, the chemical analysis results are used rather than proximate analysis and ultimate analysis.

Figure 1a shows the schematic of the pyrolysis process. With the heat provided by surrounding chamber, tobacco particles began to release gas. With the increasing temperature, more gas was released and the char and tar were formed.
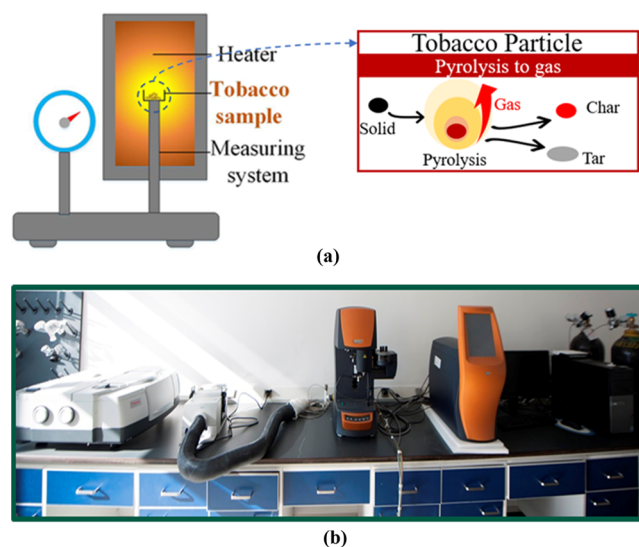

(a)

(b)

Figure 1. (a) Schematic of the pyrolysis process. (b) *Discovery* thermogravimetric analyzer produced by TA Instruments.

All of the thermogravimetric analysis (TGA) was done by the *Discovery* thermogravimetric analyzer produced by TA Instruments as shown in Figure 1b. The experiments were done in the following way. First, the tobacco samples were triturated into particles and then passed through a 178 μm diameter (80 mesh) sieve. Second, 8 mg samples were dehydrated by being heated to 473 K at a heating rate of 40 K/min from room temperature and held at that temperature for 30 min, and the weight of samples after dehydration was set as 100%. Third, the dehydrated samples were then devolatilized at different heating rates (10, 25, 50, 75, 100, 125, 150, 175, 200, 225, 250, 275, 300, 325, 350, 375, 400, 425, 450, 475, and 500 K/min in the present work) from 473 K to 1173 K, and their mass loss with the increasing temperature was recorded. All the experiments were conducted under a nitrogen atmosphere at a flow rate of 40 mL/min, and each test was repeated three times to ensure the reproducibility of the result.

In this manuscript, each major component (cellulose*, hemicellulose*, and lignin*) of the tobacco samples is obtained from the literature,[23] as both works share the same samples (Table 2). And there are full descriptions with details

Table 2. Major Components (Cellulose*, Hemicellulose*, and Lignin*) of the Tobacco Samples[23]

no.	hemicellulose* (%)	cellulose* (%)	lignin* (%)
1	25.62	6.98	45.05
2	36.07	5.65	41.89
3	23.89	6.58	46.21
4	26.49	4.29	42.20
5	26.69	6.75	47.46
6	15.20	14.93	47.48
7	25.39	5.88	42.93
8	25.96	5.22	43.44
9	27.57	4.98	45.48
10	12.26	12.48	46.18
11	31.84	4.86	45.09

in the literature;[23] for brevity, there is no discussion about those here. It is worth noting that the asterisk (*) is used to distinguish those from the common components of normal biomass.

2.2. CPD Model. The CPD model was developed by Fletcher et al.[24] for coal devolatilizations. It predicts coal devolatilization yields as a function of time, temperature, pressure, and heating rate. The CPD model considers that coal is made up of a macromolecular chain of aromatic clusters linked through chemical bridges, which have been classified as the labile bridges and the charred bridges. With the increase of temperature, the bridges (ψ) become activated (ψ^* in Figure 2) and can proceed through two competing pathways: one is to form tar (δ in Figure 2) and subsequent gas (g_1 in Figure 2) with further reaction, and the other is to form gas (g_2 in Figure 2), as well as the bridges left intact form char (c in Figure 2).
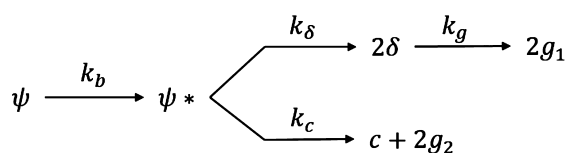

Figure 2. Reaction scheme of the CPD model.[24]

The reaction kinetics can be described by the following equations.

$$\frac{d\psi}{dt} = -k_b\psi \tag{1}$$

$$\frac{d\psi^*}{dt} = k_b\psi - (k_\delta + k_c)\psi^* \tag{2}$$

where the ψ, ψ^*, δ, g_1, g_2, and c stand for the bridges, activated bridges, tar, subsequent gas with tar, subsequent gas with char, and char.

When the reaction is close to the equilibrium state, eq 2 equals 0 and eq 3 can be derived,

$$\psi^* \cong \frac{k_b\psi}{k_\delta + k_c} \tag{3}$$

$$\frac{dc}{dt} = k_c\psi^* \cong \frac{k_bk_c\psi}{k_\delta + k_c} = \frac{k_b\psi}{\rho + 1} \tag{4}$$

in which,

$$\rho = \frac{k_\delta}{k_c} = A_\rho\, e^{(E_o \pm V_\rho)/(RT_p)} \tag{5}$$

and eq 6 can also be derived,

$$\frac{d\delta}{dt} = 2k_\delta\psi^* - k_g\delta \cong \frac{2k_gk_b\psi}{k_\delta k_c} - k_g\delta = \frac{2\rho k_b\psi}{\rho + 1} - k_g\delta \tag{6}$$

where reaction rates k_b and k_g can be calculated by the Arrhenius law,

$$k_b = A_b\, e^{(E_b \pm V_b)/(RT_p)} \tag{7}$$

$$k_g = A_g\, e^{(E_g \pm V_g)/(RT_p)} \tag{8}$$

where k_b, A_b, E_b, and V_b are the reaction rate, frequency factor, activation energy, and standard deviation of labile bridge dissociation reaction. k_g, A_g, E_g, and V_g are the reaction rate, frequency factor, activation energy, and standard deviation of gas release reaction, respectively. ρ is the composite rate constant and R is the gas constant.

There are some other equations used in the CPD model but the parameters of them are not the key parameters in the present work, so for brevity, they are not listed here and the interested readers could refer to refs 24−26.

The coal CPD model has been further extended to the Bio-CPD model by Fletcher et al.,[25,26] which has been used to predict biomass pyrolysis behavior, and good agreement compared with experimental data has been achieved.[16−18] Commonly, biomass is a term for all organic material that stems from plants (including algae, trees, and crops) and contains varying amounts of cellulose, hemicellulose, lignin, and a small number of other extractives.[27] Regarding the implementation of the Bio-CPD model, it is individually calculated for the three major components (cellulose, hemi-cellulose, and lignin) with different structural and kinetic parameters. Then, the total yield is the linear combination of each constituent component.

2.3. Toba-CPD Model. The flow map of how to build the Toba-CPD model is shown in Figure 3. The Toba-CPD model retains the general kinetic framework of the Bio-CPD model, but the kinetic parameters of the reaction routines were
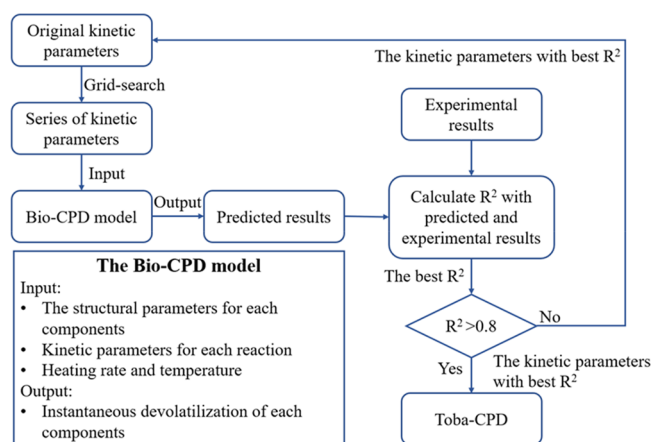
Figure 3. Flow map of the Toba-CPD model.

modified by using a grid-search optimization strategy with experimental data (various tobacco types and heating conditions) as benchmarks. In the grid-search method optimization strategy, the parameters space is meshed within certain ranges with equal adjustment steps (details will be introduced in the following paragraph). A set of parameters at each step is taken as the input parameters of the Bio-CPD model to obtain a prediction of the tobacco pyrolysis TGA profile. Then the difference between the calculated TGA and experimental TGA profiles is measured with R^2. The best R^2 among all R^2s is selected, and the situation will be different based on the value of the best R^2. If the best R^2 is larger than 0.8, the set of parameters with the best R^2 is selected as the optimal kinetic parameters of the Toba-CPD model. Otherwise, the set of parameters with the best R^2 is regarded as the new original parameters for the next loop. From the principle of the CPD model and our preliminary test results, the yield and the peak area of the derivative thermogravimetry (DTG) curve are mainly affected by the composite rate constant ρ, and the peak position of the DTG curve is mainly affected by activation energy E_b of the labile bridge dissociation reaction and activation energy E_g of gas release reaction. While the half-peak width of the DTG curve is mainly influenced by the standard deviation V_b of the bridge bond fracture reaction and the standard deviation V_g of the gas release reaction.

According to the preliminary test of adjusting parameters, and considering both the accuracy and the cost of the calculation, the parameters E_b, E_g, V_b, V_g, and ρ are chosen to be adjusted in the present work. The searching space for ρ is set as ±25% of the standard value in the Bio-CPD model, and the searching spaces for E_b, E_g, V_b, and V_g are set as ±40% of the standard value in the Bio-CPD model, and the searching steps for all parameters are set as 10 for each loop. And it is worth noting that the selection of parameters space and step are not empirical; we determined the parameters space and step after a trial-and-error pretest.

3. RESULTS AND DISCUSSION

In this section, we first present the *a priori* analysis result of the Bio-CPD model for tobacco pyrolysis. Then the results of the

Table 3. Kinetic Parameters of the Specific Toba-CPD Model for Tobacco Sample No. 1

parameter	cellulose*	hemicellulose*	lignin*
E_b(kJ/mol)	47.7	55.479	60.388
A_b (s^{-1})	2.1×10^{15}	1.2×10^{20}	7.04×10^{16}
V_b(kJ/mol)	0.54	2.096	9.809
E_g(kJ/mol)	46.805	43.616	64.125
A_g (s^{-1})	3×10^{15}	3×10^{15}	2.3×10^{19}
V_g(kJ/mol)	2.97	5.408	12.422
ρ(−)	1.35	1.57	1.72

Toba-CPD model, including the Toba-CPD model for a certain tobacco and the general Toba-CPD model for a wide range of tobacco samples are introduced step-by-step.

3.1. *A Priori* Study on the Bio-CPD Model for Tobacco Pyrolysis. Figure 4 shows comparisons of experimental results and the predictions of the Bio-CPD model for each major component (cellulose*, hemicellulose*, and lignin*), and their mixture for tobacco sample No. 1. Based on the principle of Bio-CPD, the sample's pyrolysis result is the linear combination of each constituent components. The subfigure on the right bottom is titled with the tobacco*, which is the total yield calculated by the linear superposition with cellulose*, hemicellulose*, and lignin*. The dark dots stand for the experiment result, and the blue lines are the result of the Bio-CPD model. As mentioned before, present work
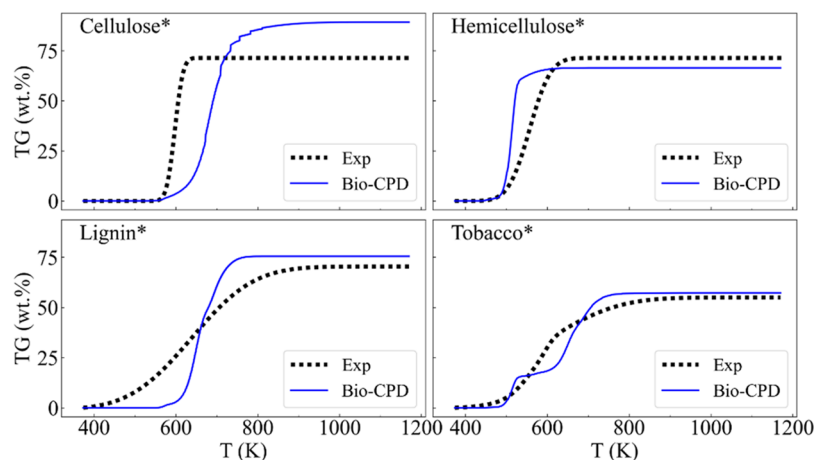

Figure 4. Comparisons of experimental results with and the predictions of the Bio-CPD model for each major component (cellulose*, hemicellulose*, and lignin*) and their mixture (tobacco*) for sample no. 1.
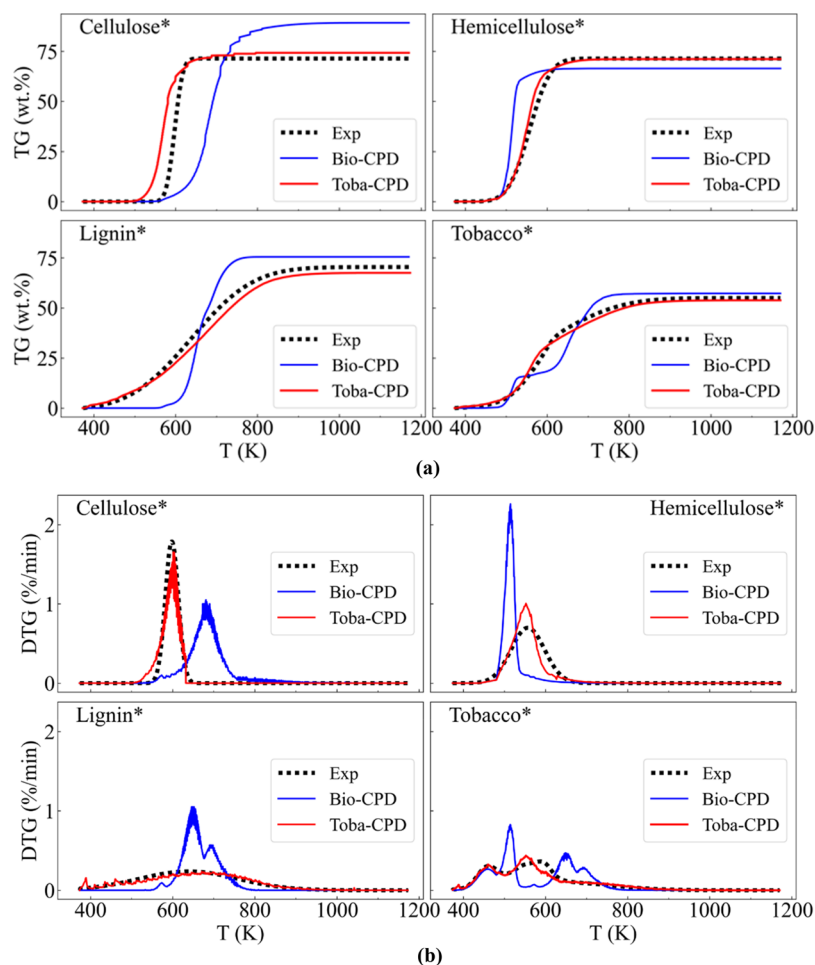
Figure 5. Comparison of experimental results and predictions of the Bio-CPD and Toba-CPD models for tobacco no. 1 at 10 K/min: (a) TG, (b) DTG.

Table 4. Kinetic Parameters of the Specific Toba-CPD Model for Tobacco No. 2

parameter	cellulose*	hemicellulose*	lignin*
E_b(kJ/mol)	44.685	51.879	48.727
A_b (s^{-1})	2.1×10^{15}	1.2×10^{20}	7.0×10^{16}
V_b(kJ/mol)	0.135	4.396	7.258
E_g(kJ/mol)	46.816	27.695	64.125
A_g (s^{-1})	3×10^{15}	3×10^{15}	2.3×10^{19}
V_g(kJ/mol)	0.972	6.708	11.969
ρ(−)	1.28	2.02	1.72

$$RMSE = \left(\frac{1}{N} \sum_{i=1}^{N} (y^{(i)}_{exp} - y^{(i)}_{pred})^2 \right)^{1/2} \quad (10)$$

where $y^{(i)}_{exp}$ is the experimental value, $y^{(i)}_{pred}$ is the predicted value and $\hat{y}_{exp}$ is the average experimental value.

As mentioned before, compared with the CPD model, the Bio-CPD model retains the same reaction schemes, but the structural parameters are modified for each component, and reaction kinetics are also performed by considering the three components' reactions. Those changes made the Bio-CPD model suitable for typical lignocellulosic biomass like Sawdust.[25] Therefore, based on the same logic, the present work developed the Toba-CPD model by modifying the reaction kinetics of the three major components based on the same reaction scheme and structural parameters of the Bio-CPD model.

3.2. Toba-CPD Model for a Specific Tobacco. To establish the Toba-CPD model for a specific tobacco, the pyrolysis data of tobacco no. 1 at various heating rates (starting from 25 to 500 K/min with a step of 25 K/min, the experimental results at 10 K/min are used for evaluating) are set as the input data for parameter searching. Table 3 lists the optimal sets of kinetic parameters for cellulose, hemicellulose, and lignin after parameter searching.

After the optimal reaction kinetic parameters are obtained, the parameters are taken into the model, and then applied to

focuses on modeling three components (hemicellulose*, cellulose*, and lignin*), where the direct comparisons with the Bio-CPD model are achieved. The results show that the Bio-CPD model would give large deviations in predicting the pyrolysis process of each component, especially for cellulose* and lignin*. The R^2/RMSE (root mean square error) of the predictions for cellulose*, hemicellulose*, lignin*, and tobacco* are 0.529/21.398, 0.862/10.206, 0.847/10.359, and 0.946/4.857 respectively, calculated by eqs 9 and 10.

$$R^2 = 1 - \frac{\sum_{i=1}^{N} (y^{(i)}_{pred} - y^{(i)}_{exp})^2}{\sum_{i=1}^{N} (y^{(i)}_{exp} - \hat{y}_{exp})^2} \quad (9)$$
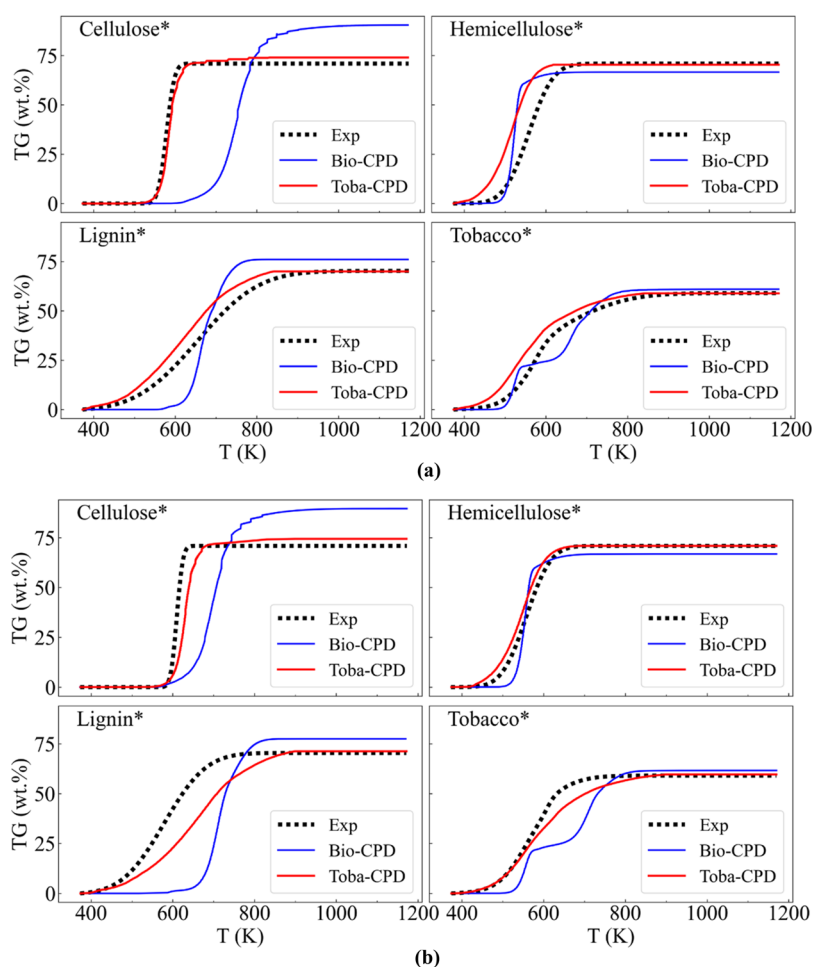
Figure 6. Comparisons of experimental results and predictions of the Bio-CPD and Toba-CPD models for tobacco no. 2 at (a) 25 K/min, and (b) 475 K/min.

predict the pyrolysis behavior of tobacco no. 1 at 10 K/min, which is unseen during parameter searching. Figure 5(a) shows the comparisons of the TG results measured from experiments and predicted by the Bio-CPD and Toba-CPD models, in which dark dots stand for the experiment result, and the red and blue lines stand for the Toba-CPD and Bio-CPD predictions, respectively. Figure 5(b) shows the comparisons of the DTG profiles. The DTG curve is obtained by temperature differentiation of the TG curve. Table 5 lists the R^2 and the RMSE of the Bio-CPD and Toba-CPD models' prediction. Obviously, compared with the Bio-CPD model, the Toba-CPD model for a specific tobacco is more accurate. The R^2 of the Toba-CPD predictions are 0.928, 0.995, 0.985, and 0.994 for cellulose*, hemicellulose*, lignin*, and tobacco*, respectively. All of them are very close to 1. The RMSE of Toba-CPD is 8,376, 2.013, 3.276, and 1.634 for cellulose*, hemicellulose*, lignin*, and tobacco*, respectively. On the contrary, R^2/RMSE of the Bio-CPD model's prediction is 0.529/21.398, 0.862/10.206, 0.847/10.357, 0.946/4.787 for cellulose*, hemicellulose*, lignin* and tobacco*, respectively. All R^2s (or RMSEs) are smaller (or larger) than those of the Toba-CPD predictions. From Figure 5(a), the curve of tobacco* from the Toba-CPD model for a specific tobacco is quite smooth and is in good agreement with the experimental curve, but that of the Bio-CPD model is quite uneven and far from the experiment curve. It is worth noting that the R^2 of the Bio-CPD model for tobacco* is better than that for each

component. This occurs because adding the results of the three components will reduce the error. Some results of the Bio-CPD model may be larger than the experiment results such as that for cellulose*, while the others may be smaller than the experiment results such as that for lignin*, and when adding them together, the error will be reduced. But it can be seen from Figure 5(a) that the curve is quite uneven and far from the experiment curve.

The Toba-CPD model performs better than the Bio-CPD model which can also be seen in Figure 5(b). In Figure 5(b), the abscissa corresponding to the maximum point of the pyrolysis rate is the characteristic temperature of the subpeak, which is also called the pyrolysis temperature. The area of peaks refers to the mass ratios of the corresponding components. It shows that the predictions of the Toba-CPD model agree well with the experimental results. It is interesting to find that the DTG curves of the cellulose frequently show a sharper peak than that of hemicellulose and lignin, which conforms to the results from the literature[28] and proves the accuracy of the Toba-CPD model. Because the DTG results are calculated from the TG results, for brevity, we only show the TG results in the following part. We believe Toba-CPD performs much better than Bio-CPD due to the optimization of kinetic parameters. After the grid-research optimization method based on a large number of experimental data, the proper kinetic parameters for tobacco have been found, resulting in a better performance of Toba-CPD.

Table 5. R^2 and RMSE of Bio-CPD and Specific Toba-CPD Model Predictions

no.	heating rate	model	cellulose*	hemicellulose*	lignin*	tobacco*
				R^2		
1	10	Toba-CPD	0.928	0.995	0.985	0.994
		Bio-CPD	0.529	0.862	0.847	0.946
2	25	Toba-CPD	0.989	0.891	0.964	0.965
		Bio-CPD	−0.058	0.799	0.847	0.938
2	475	Toba-CPD	0.950	0.989	0.859	0.957
		Bio-CPD	0.519	0.964	0.290	0.705
				RMSE		
1	10	Toba-CPD	8.376	2.013	3.276	1.634
		Bio-CPD	21.398	10.206	10.359	4.787
2	25	Toba-CPD	3.114	8.708	5.087	3.851
		Bio-CPD	30.877	8.463	10.527	5.106
2	475	Toba-CPD	7.078	2.872	9.725	4.293
		Bio-CPD	21.990	5.112	21.809	11.181

Table 6. Kinetic Parameters of the General Toba-CPD Model Obtained from Parameter Searching

parameter	cellulose*	hemicellulose*	lignin*
E_b(kJ/mol)	39.559	53.584	54.139
A_b (s^{-1})	2.1×10^{15}	1.2×10^{20}	7.0×10^{16}
V_b(kJ/mol)	1.471	3.728	7.581
E_g(kJ/mol)	34.925	22.863	58.206
A_g (s^{-1})	3×10^{15}	3×10^{15}	2.3×10^{19}
V_g(kJ/mol)	1.438	5.393	10.296
$\rho(-)$	1.37	1.99	1.56

After verifying the feasibility of our grid-search method optimization strategy in optimizing kinetic parameters for Toba-CPD, the following part will test the model's performance on different heating rates. The pyrolysis data of tobacco no. 2 at different heating rates (starting from 10 to 500 K/min with a step of 25 K/min except for 20 and 475 K/min) are chosen as the input data for parameter searching by a grid-research optimization method. Table 4 lists the results of the parameter searching.

After the reaction kinetic parameters are obtained, the parameters are taken into the model and then applied to predict the devolatilization process of tobacco no. 2 at 25 and 475 K/min. These parameter values are used for evaluating the model and have not been input during parameter searching. The results are shown in Figure 6.

Figure 6 shows the comparisons of the TG results of tobacco no. 2 at 25 K/min (a) and at 475 K/min (b) predicted with the Bio-CPD and Toba-CPD models, in which the same labels in Figure 6 are used. It can be the seen that Toba-CPD model still performs better than Bio-CPD of tobacco no. 2 at both low (25 K/min) and high (475 K/min) heating rates. From Table 5, the R^2 values of the Toba-CPD model are 0.989, 0.891, 0.964, and 0.965 for cellulose*, hemicellulose*, lignin*

and tobacco* at 25 K/min, respectively, and those at 475 K/min are 0.95, 0.989, 0.859 and 0.957, respectively. All of them are very close to 1 and larger than those of the Bio-CPD model, which are −0.058, 0.799, 0.574, and 0.938 at 25 K/min, and are 0.519, 0.964, 0.290, and 0.705 at 475 K/min. The error of the Bio-CPD model is quite large, especially for the cellulose of tobacco no. 2 at 25 K/min, for which R^2 equals −0.058, even less than 0. Also, similar to the previous, R^2 of tobacco* of the Bio-CPD model is larger than that of the individual components because adding the results of the three components will reduce the error.

From all above, it can be concluded that the Toba-CPD model for a specific tobacco is much better than the traditional Bio-CPD model and is capable of modeling the pyrolysis of specific tobaccos under different heating rates. We will now further develop the general Toba-CPD model for various tobacco types in the next section.

3.3. General Toba-CPD Model for Various Tobaccos. After confirming the feasibility of the Toba-CPD model for a specific tobacco, a general Toba-CPD model is further developed for various tobacco types. Like before, the pyrolysis data of all tobaccos at various heating rates (starting from 10 to 500 K/min with a step of 25 K/min except for tobacco no. 1 at 50 K/min and tobacco no. 11 at all heating rates) are used as the input data for parameter searching. Table 6 lists the results from parameter searching.

After the optimal reaction kinetic parameters are obtained, the parameters are taken into the model, and then applied to predict the pyrolysis behavior of tobacco no. 1 at 50 K/min and tobacco no. 11 at 100 K/min, which are unseen during parameter searching. The results are shown in Figure 7.

Figure 7 shows the comparison of experimental results and predictions of the Bio-CPD model and the general Toba-CPD model for tobacco no. 1 at 50 K/min(a), and tobacco no. 11 at 100 K/min (b). The labels are the same as those in Figure 5. Table 7 lists R^2 and RMSE values of the predictions of the Bio-CPD and Toba-CPD models against the experiment. The R^2/RMSE values of the Toba-CPD model are 0.998/1.248, 0.976/4.343, 0.981/3.657, and 0.987/2.376 for cellulose*, hemicellulose*, lignin*, and tobacco* for tobacco no. 1 at 50 K/min, respectively, and those for tobacco no. 11 at 100 K/min are 0.995/2.375, 0.958/5.693, 0.980/3.663, and 0.985/2.834, respectively. All their R^2 values are very close to 1, and RMSEs are quite small. From Figure 7, the curves of Toba-CPD on tobacco* are also close to the experimental curves. It is worth noting there no pyrolysis data of tobacco no. 11 had been inputted for parameter searching, which is totally new for the model. On the contrary, other parameters searching are performed only without inputting the pyrolysis data at a certain heating rate. So, the general Toba-CPD's performance on tobacco no. 11 can prove the generality of the Toba-CPD model, and it is quite good with R^2 equaling 0.985, RMSE equaling 2.584, and the curves being very similar to the experimental curve. From what has been discussed above, we can reasonably arrive at the conclusion that the general Toba-CPD model is able to model tobacco pyrolysis and is much better than the Bio-CPD model for tobacco pyrolysis.

Then, we further compare the specific Toba-CPD with the general Toba-CPD. Figure 8 shows the TG results of specific Toba-CPD and general Toba-CPD of tobacco no. 1 at 10 k/min, in which dark dots stand for the experiment result, and the red line, green line, and blue line stand for specific Toba-CPD, general Toba-CPD, and Bio-CPD, respectively. It is hard
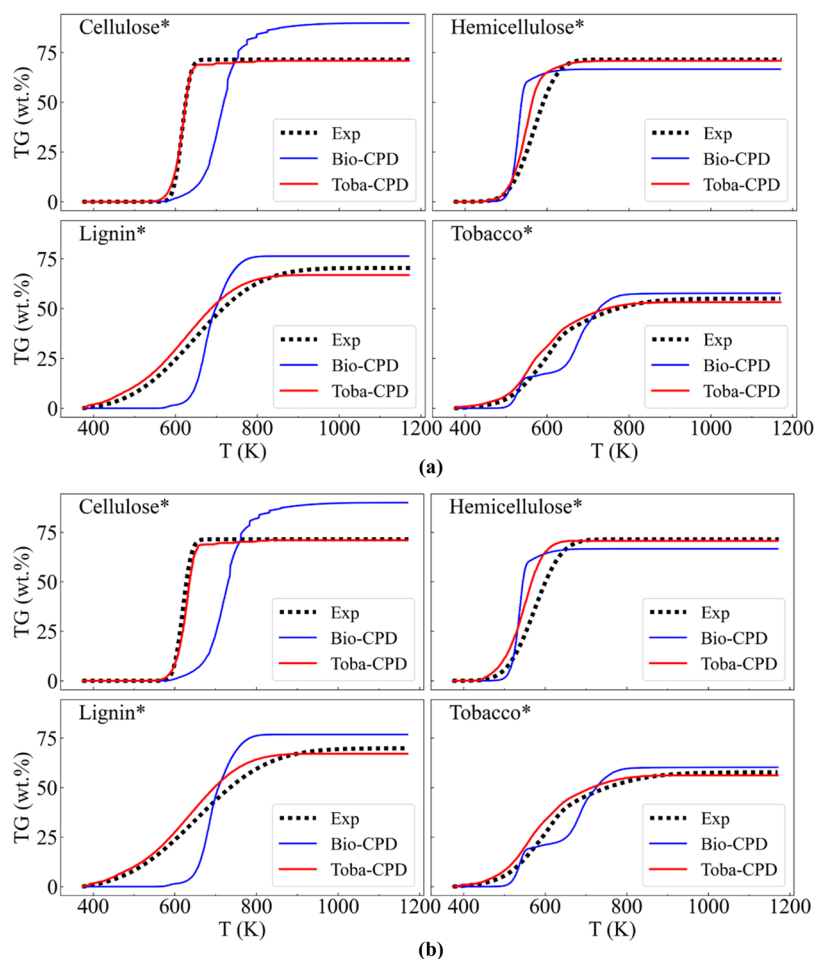
Figure 7. Comparisons of experimental results and predictions of the Bio-CPD model and the general Toba-CPD model for tobacco no. 1 at 50 K/min (a), and tobacco no. 11 at 100 K/min (b).

Table 7. R^2 and RMSE of Bio-CPD and General Toba-CPD Models Prediction

no.	heating rate	model	cellulose*	hemicellulose*	lignin*	tobacco*
			R^2			
1	50	Toba-CPD	0.998	0.976	0.981	0.987
		Bio-CPD	0.521	0.896	0.814	0.934
1	10	Toba-CPD	0.968	0.979	0.987	0.991
		Bio-CPD	0.529	0.862	0.847	0.946
11	100	Toba-CPD	0.995	0.958	0.980	0.983
		Bio-CPD	0.479	0.905	0.762	0.940
			RMSE			
1	50	Toba-CPD	1.248	4.343	3.657	2.376
		Bio-CPD	22.106	8.971	11.423	5.367
1	10	Toba-CPD	5.583	3.980	3.041	1.974
		Bio-CPD	21.398	10.206	10.359	4.787
11	100	Toba-CPD	2.375	5.693	3.663	2.834
		Bio-CPD	23.123	8.556	12.567	5.271

to tell which model performs better only on the figure; both models (specific Toba-CPD and the general Toba-CPD) show similar behaviors. The R^2 of specific Toba-CPD is 0.998, 0.976, 0.981, and 0.987 for cellulose*, hemicellulose*, lignin*, and tobacco* for tobacco no. 1 at 10 K/min, respectively, and those of general Toba-CPD are 0.928, 0.995, 0.985, and 0.994. While the RMSE of specific Toba-CPD for tobacco* is 1.634 and that of general Toba-CPD is 1.974. From the comparison of R^2 and RMSE, specific Toba-CPD is slightly better than

general Toba-CPD. Hence, it can be concluded that the general model can predict tobacco pyrolysis at a high accuracy, which is close to specific Toba-CPD in accuracy but with more generality.

The Toba-CPD model currently has potential limitations. First, the heating rate range of the experimental equipment used in our study (The *Discovery* thermogravimetric analyzer produced by TA Instruments) cannot exceed 500 K/min, so only the experiment under 500 K/min can be done. Second, in
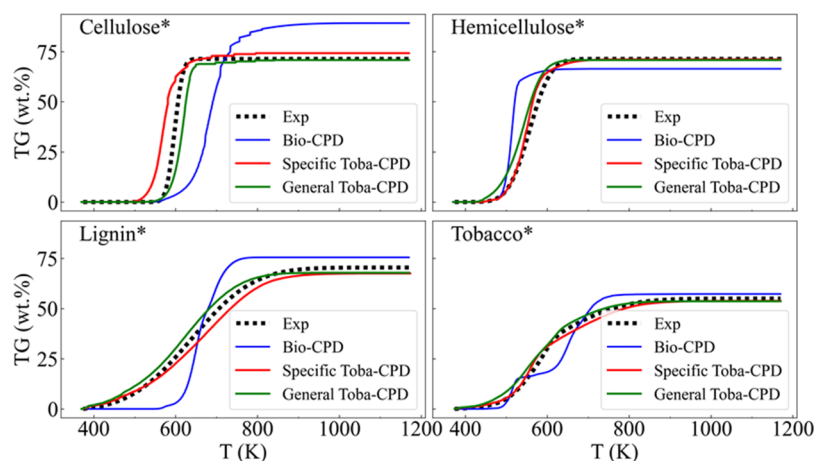
Figure 8. Comparison of experiment results with Bio-CPD, specific Toba-CPD, and general Toba-CPD of tobacco no. 1 at 10 K/min

the present work, the proper kinetic parameters for Toba-CPD have been found, but the percentage of each component of tobacco is still needed for calculating the sample's pyrolysis with the linear combination of each constituent components. In the future work, we will try to find the relation between chemical analysis and percentage of each component.

4. CONCLUSION

This work first studied the performance of Bio-CPD model in predicting tobacco pyrolysis, and the result showed that the Bio-CPD model would give large deviations in modeling tobacco pyrolysis. So, we further extended the Bio-CPD model for tobacco pyrolysis, that is the Toba-CPD model. In the Toba-CPD model, the general kinetic framework of the Bio-Chemical Percolation Devolatilization (Bio-CPD) model was retained, but the kinetic parameters of the reaction routines were modified by using a grid-search optimization strategy with experimental data (various tobacco types and heating conditions) as benchmarks. First, the pyrolysis process of 11 kinds of tobacco under a wide range of heating rates (10−500 K/min) was measured through TGA. The collected TGA data were then divided into the seen and unseen data sets for the model development and validation. Second, the performance of the Bio-CPD model on tobacco pyrolysis was assessed through the *a priori* study on the established database. The results showed that the traditional Bio-CPD model would give large deviations in predicting the tobacco pyrolysis (both final volatiles yield and pyrolysis process). Finally, the Toba-CPD models for a specific tobacco and for all tobacco were developed. The performance of models were further evaluated on the unseen tobacco and heating conditions. It was demonstrated that the developed Toba-CPD model could well reproduce the tobacco pyrolysis process for various tobacco types under a wide range of heating rates ($R^2 > 0.992$).

AUTHOR INFORMATION

Corresponding Authors

Jiangkuan Xing − *State Key Laboratory of Clean Energy Utilization, Zhejiang University, Hangzhou 310027, P. R. China; Department of Mechanical Engineering and Science, Kyoto University, Kyoto 615-8540, Japan;* ● orcid.org/0000-0002-2423-5627; Email: zjuxjk@zju.edu.cn

Kun Luo − *State Key Laboratory of Clean Energy Utilization, Zhejiang University, Hangzhou 310027, P. R. China;*

● orcid.org/0000-0003-3644-9400; Phone: 86-571-87951764; Email: zjulk@zju.edu.cn

Authors

Hao Wei − *State Key Laboratory of Clean Energy Utilization, Zhejiang University, Hangzhou 310027, P. R. China*

Yuhan Peng − *China Tobacco Zhejiang Industrial Co., Ltd., Hangzhou 310088, P. R. China*

Hua Huang − *China Tobacco Zhejiang Industrial Co., Ltd., Hangzhou 310088, P. R. China*

Jianqi Fan − *State Key Laboratory of Clean Energy Utilization, Zhejiang University, Hangzhou 310027, P. R. China*

Jianren Fan − *State Key Laboratory of Clean Energy Utilization, Zhejiang University, Hangzhou 310027, P. R. China;* ● orcid.org/0000-0002-6332-6441

Lu Dai − *China Tobacco Zhejiang Industrial Co., Ltd., Hangzhou 310088, P. R. China*

Complete contact information is available at:
https://pubs.acs.org/10.1021/acsomega.2c05098

Notes

The authors declare no competing financial interest.

■ ACKNOWLEDGMENTS

■ REFERENCES

(1) *Tobacco industry*. Statista. https://www.statista.com/topics/1593/tobacco/ (accessed 2022-03-25).

(2) Hammond, D. Health Warning Messages on Tobacco Products: A Review. *Tobacco Control* **2011**, *20* (5), 327−337.

(3) Xing, J.; Luo, K.; Wang, H.; Jin, T.; Fan, J. Novel Sensitivity Study for Biomass Directional Devolatilization by Random Forest Models. *Energy Fuels* **2020**, *34* (7), 8414−8423.

(4) Wei, H.; Luo, K.; Xing, J.; Fan, J. Predicting Co-Pyrolysis of Coal and Biomass Using Machine Learning Approaches. *Fuel* **2022**, *310*, 122248.

(5) Trubetskaya, A.*Fast Pyrolysis of Biomass at High Temperatures*. Ph.D. Thesis, Technical University of Denmark, 2016.

(6) Davis, D. L.; Nielsen, M. T.*Tobacco: Production, Chemistry, and Technology*; Wiley, 1999.

(7) Baker, R. R.; Bishop, L. J. The Pyrolysis of Tobacco Ingredients. *Journal of Analytical and Applied Pyrolysis* **2004**, *71* (1), 223−311.

(8) Peng, Y.; Hao, X.; Qi, Q.; Tang, X.; Mu, Y.; Zhang, L.; Liao, F.; Li, H.; Shen, Y.; Du, F.; Luo, K.; Wang, H. The Effect of Oxygen on In-Situ Evolution of Chemical Structures during the Autothermal Process of Tobacco. *Journal of Analytical and Applied Pyrolysis* **2021**, *159*, 105321.

(9) Liu, B.; Li, Y.-M.; Wu, S.-B.; Li, Y.-H.; Deng, S.-S.; Xia, Z.-L. Pyrolysis Characteristic of Tobacco Stem Studied by Py-GC/MS, TG-FTIR, and TG-MS. *BioResources* **2012**, *8* (1), 220−230.

(10) Barontini, F.; Tugnoli, A.; Cozzani, V.; Tetteh, J.; Jarriault, M.; Zinovik, I. Volatile Products Formed in the Thermal Decomposition of a Tobacco Substrate. *Ind. Eng. Chem. Res.* **2013**, *52* (42), 14984−14997.

(11) Calabuig, E.; Juárez-Serrano, N.; Marcilla, A. TG-FTIR Study of Evolved Gas in the Decomposition of Different Types of Tobacco. Effect of the Addition of SBA-15. *Thermochim. Acta* **2019**, *671*, 209−219.

(12) Guo, G.; Liu, C.; Wang, Y.; Xie, S.; Zhang, K.; Chen, L.; Zhu, W.; Ding, M. Comparative Investigation on Thermal Degradation of Flue-Cured Tobacco with Different Particle Sizes by a Macro-Thermogravimetric Analyzer and Their Apparent Kinetics Based on Distributed Activation Energy Model. *J. Therm Anal Calorim* **2019**, *138* (5), 3375−3388.

(13) Chen, P. A Mathematical Model of Cigarette Smoldering Process. *Beiträge zur Tabakforschung International/Contributions to Tobacco Research* **2002**, *20* (4), 265−271.

(14) Encinar, J. M.; Beltrán, F. J.; González, J. F.; Moreno, M. J. Pyrolysis of Maize, Sunflower, Grape and Tobacco Residues. *J. Chem. Technol. Biotechnol.* **1997**, *70* (4), 400−410.

(15) Gao, W.; Chen, K.; Xiang, Z.; Yang, F.; Zeng, J.; Li, J.; Yang, R.; Rao, G.; Tao, H. Kinetic Study on Pyrolysis of Tobacco Residues from the Cigarette Industry. *Industrial Crops and Products* **2013**, *44*, 152−157.

(16) Zhang, J.; Zheng, S.; Chen, C.; Wang, X.; ur Rahman, Z.; Tan, H. Kinetic Model Study on Biomass Pyrolysis and CFD Application by Using Pseudo-Bio-CPD Model. *Fuel* **2021**, *293*, 120266.

(17) Wan, K.; Wang, Z.; He, Y.; Xia, J.; Zhou, Z.; Zhou, J.; Cen, K. Experimental and Modeling Study of Pyrolysis of Coal, Biomass and Blended Coal-Biomass Particles. *Fuel* **2015**, *139*, 356−364.

(18) Rabaçal, M.; Costa, M.; Vascellari, M.; Hasse, C.; Rieth, M.; Kempf, A. M. A Large Eddy Simulation Study on the Effect of Devolatilization Modelling and Char Combustion Mode Modelling on the Structure of a Large-Scale, Biomass and Coal Co-Fired Flame. *Journal of Combustion* **2018**, *2018*, 1−15.

(19) Chen, Y.; Charpenay, S.; Jensen, A.; Wójtowicz, M. A.; Serio, M. A. Modeling of Biomass Pyrolysis Kinetics. *Symposium (International) on Combustion* **1998**, *27* (1), 1327−1334.

(20) Niksa, S. Bio-FLASHCHAIN® Theory for Rapid Devolatilization of Biomass 2. Predicting Total Yields for Torrefied Woods. *Fuel* **2020**, *263*, 116645.

(21) Sheng, C.; Azevedo, J. L. T. Modeling Biomass Devolatilization Using the Chemical Percolation Devolatilization Model for the Main Components. *Proceedings of the Combustion Institute* **2002**, *29* (1), 407−414.

(22) Fletcher, T. H. Review of 30 Years of Research Using the Chemical Percolation Devolatilization Model. *Energy Fuels* **2019**, *33* (12), 12123−12153.

(23) Mu, Y.; Peng, Y.; Tang, X.; Ren, J.; Xing, J.; Luo, K.; Fan, J.; Zhang, K. Experimental and Kinetic Studies on Tobacco Pyrolysis under a Wide Range of Heating Rates. *ACS Omega* **2022**, *7*, 1420.

(24) Fletcher, T. H.; Kerstein, A. R.; Pugmire, R. J.; Grant, D. M. Chemical Percolation Model for Devolatilization. 2. Temperature and Heating Rate Effects on Product Yields. *Energy Fuels* **1990**, *4* (1), 54−60.

(25) Lewis, A. D.; Fletcher, T. H. Prediction of Sawdust Pyrolysis Yields from a Flat-Flame Burner Using the CPD Model. *Energy Fuels* **2013**, *27* (2), 942−953.

(26) Fletcher, T. H.; Pond, H. R.; Webster, J.; Wooters, J.; Baxter, L. L. Prediction of Tar and Light Gas during Pyrolysis of Black Liquor and Biomass. *Energy Fuels* **2012**, *26* (6), 3381−3387.

(27) McKendry, P. Energy Production from Biomass (Part 1): Overview of Biomass. *Bioresour. Technol.* **2002**, *83* (1), 37−46.

(28) Várhegyi, G.; Chen, H.; Godoy, S. Thermal Decomposition of Wheat, Oat, Barley, and Brassica Carinata Straws. A Kinetic Study. *Energy Fuels* **2009**, *23* (2), 646−652.